Optical properties of ferroelectric nanocrystal-containing polymer BaTiO₃/polycarbonate films

W. C. Liu
National Laboratory of Solid State Microstructures and Department of Materials Science and Engineering, Nanjing University, Nanjing 210093, People's Republic of China and Department of Applied Physics and Materials Research Center, Hong Kong Polytechnic University, Hung Hom, Hong Kong, People's Republic of China

A. D. Li[a)] and J. Tan
National Laboratory of Solid State Microstructures and Department of Materials Science and Engineering, Nanjing University, Nanjing 210093, People's Republic of China

C. L. Mak and K. H. Wong
Department of Applied Physics and Materials Research Center, Hong Kong Polytechnic University, Hung Hom, Hong Kong, People's Republic of China

D. Wu and Nai-Ben Ming
National Laboratory of Solid State Microstructures and Department of Materials Science and Engineering, Nanjing University, Nanjing 210093, People's Republic of China

BaTiO₃ (BT)-nanocrystal-doped polycarbonate polymer composite thin films (BT/PC) with different BT concentrations were prepared by spin-coating method. Ultrafine BT (~40–50 nm) nanocrystals with pure perovskite tetragonal phase were synthesized by hydrothermal method. The structure of BT nanocrystals and composite films were studied by means of x-ray diffraction and transmission scanning microscopy. The composite films were poled with a high electric field at a suitable temperature to yield a noncentrosymmetric arrangement and produce better electro-optic properties. The poling condition under external electric field was optimized through the dielectric properties of BT and PC polymer and the effective-field intensity theory. The electro-optic (EO) coefficients and transmittance of composite films with various BT concentrations were also evaluated. The average effective linear EO coefficient and figure of merit of 20-wt % BT-doped composite films were about 63.1 and 103.1 pm/V, respectively. BT/PC composite films show excellent electro-optic properties for application in integrated optoelectronics and optics. © *2005 American Institute of Physics.* [DOI: 10.1063/1.1984076]

I. INTRODUCTION

Many ferroelectric materials such as BaTiO₃ (BT), Sr₂₋ₓCaₓNaNb₅O₁₅ (SCNN), and Pb(Zr₁₋ₓTiₓ)O₃ (PZT) are potentially superior for electro-optic, nonlinear optic, and photorefractive applications due to their many outstanding properties such as extremely high electro-optic (EO) and nonlinear optical (NLO) coefficients.[1–3] Perovskite BaTiO₃, with the simplest structure in oxygen octahedral ferroelectric materials and large effective EO coefficient, becomes one of the most widely studied materials and some optical applications made of it were fabricated.[4,5] However, the growth of large, perfect, and pure ferroelectric crystals has proven to be very difficult. Additionally, the ferroelectric single crystals are normally very expensive, most of which are uneconomical in commercial application. All of these prevent these materials from being used widely in industry. In past decades, optical organic polymers have received considerable attention because of their advantages such as low dielectric constant, quick response, high transparency, and simple manufacture.[6–8] The ferroelectric nanocrystal/polymer com-

posite films, combining both the merit of ferroelectric materials and polymers, especially their very large electro-optic figure of merit $F_2 = n^3\gamma/\epsilon$, an important parameter for optical device materials, become one of the most promising materials in the field of EO and NLO optics.[9] Normally, the orientations of nanometer particles as active particles in composite films are random before poling, so an appropriate electric field is needed to make these active particles align in such a way that the total system is noncentrosymmetric. In this paper, using BaTiO₃ nanocrystals as optical active units and polycarbonate (PC) as host polymer material, we prepared different volume concentrations BT-doped composite films and mainly investigated the poling condition, transmission properties, and EO properties of the poled composite polymer thin films.

II. EXPERIMENT

A. BT nanocrystal synthesis and polymer film preparation

The hydrothermal method was chosen to prepare high-quality BT ultrafine crystals due to its advantages such as a low-temperature process, environmental friendliness, and precise control in compositions.[10] The raw materials were

---

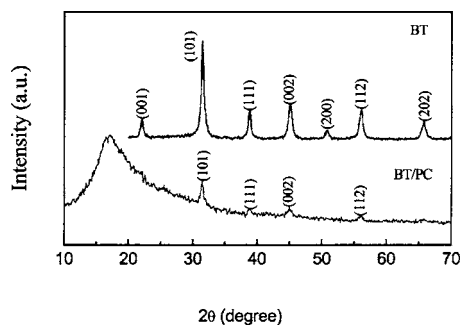a)Author to whom correspondence should be addressed; FAX: +86-025-83595535; electronic mail: adli@netra.nju.edu.cn

FIG. 1. XRD patterns of BT nanocrystals and BT/PC composite films.

FIG. 2. The TEM photograph of BT nanocrystals prepared by hydrothermal method.

barium nitrate $[Ba(NO_3)_2]$ and titanium tetrachloride $(TiCl_4)$. First, $Ba(NO_3)_2$ was dissolved in de-ionized water, then stoichiometric $TiCl_4$ and a proper amount of KOH was added into the $Ba(NO_3)_2$ solution quickly at the same time. After being stirred for 1 h and filtered, the starchy sediment was added in 10-mol/l KOH solution. The resultant precursor was heated in a 50-ml capacity Teflon-lined Parr vessel at 140 °C for 12 h. After filtration and washing, the needed BT nanocrystals were obtained. The BT/PC composite thin films were prepared by spin-coating method. PC polymer was dissolved in chloroform. The mixed BT nanocrystals/PC precursor solution was synthesized by dispersing BT nanocrystals into the above PC solution. The weight ratio of BT to PC in the composite films was very low (5%, 10%, and 20%, respectively). Ultrasonic stirring was used to ensure uniform BT nanocrystal incorporation in the mixed solution. BT/PC composite films were deposited on quartz or commercial indium-tin oxide (ITO) glass substrates by the spin-coating technique at 2500 rpm for 20 s. As-deposited wet films were baked at 60 °C for 10 min to remove the chloroform solvent. The procedure was repeated several times to obtain the needed thick films. At last the films were baked at 60 °C for 2 h at air. Typical film thickness is ~1.2 μm with four-layer depositions.

B. Characterization of BT nanocrystals and BT/PC polymer films

The crystallinity and structure of BT nanocrystals and BT/PC composite films were characterized by x-ray diffraction (XRD) with Cu K_α radiation. The size and shape of BT particles were observed using the transmission electron microscopy (TEM). The composite films were poled by using corona-onset poling at elevated temperature (COPET). The transmittances of the composite films before and after poling were examined by a recording UV-visible spectrometer. The dielectric constant of the composite films was measured by the precise impedance analyzer Agilent 4294A. The average EO coefficients of the composite films were detected using the film birefringence EO measurement method.

III. RESULTS AND DISCUSSION

A. Structure and morphology of BT nanocrystals and BT/PC composite films

Figure 1 shows the XRD patterns of BT nanocrystals and BT/PC composite films. It is easily seen that the BT ultrafine
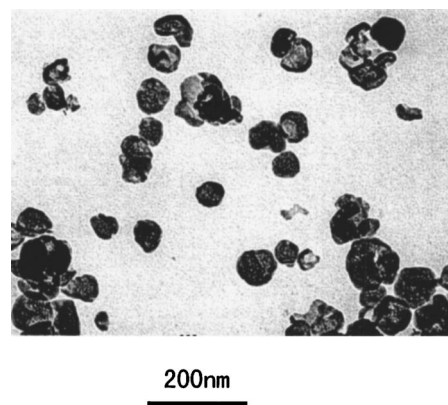
particles prepared by hydrothermal method have pure tetragonal perovskite structure without a secondary phase. Compared to the pattern of BT powders, the peak intensity and quantity of the BT/PC films are decreased significantly due to the low BT content, amorphous glass substrate, and polymer matrix. However, the strongest (101) BT peak can still be recognized clearly. The BT ultrafine powders prepared by hydrothermal method exhibit spheroid or ellipse shapes with an average size of ~40–50 nm, as confirmed by the TEM image in Fig. 2.

B. Poling and optical properties of BT/PC composite films

To measure the electro-optic (EO) coefficient, planar parallel electrodes were deposited on top of the film. A suitable electric field was applied to the films at an elevated temperature to make the nanocrystals align. Since the concentration of BT nanocrystals in composite thin films is low and the shapes of BT nanocrystals observed by TEM are
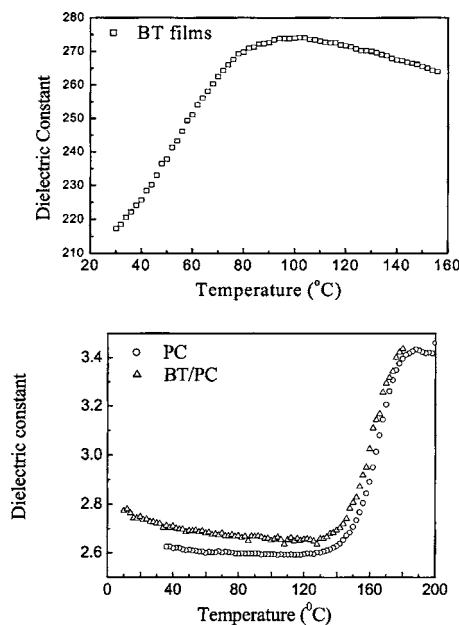

FIG. 3. The dielectric constant-temperature spectra of BT films, PC, and 10% BT-doped composite films with a ramp rate of 2 °C/min.
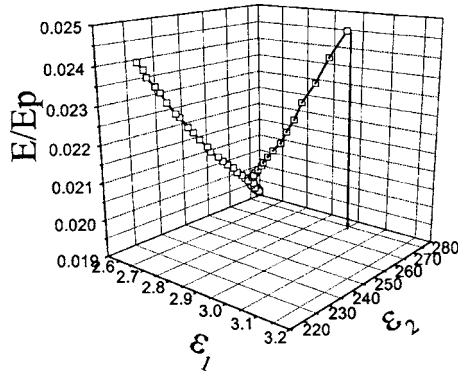
FIG. 4. The dependence of E/E_p on dielectric constants of PC (ϵ_1) and BT (ϵ_2).

FIG. 6. Plots of $(\alpha h\nu)^{1/2}$ as a function of $h\nu$ for BT/PC films. Extrapolating the line to intersect with the energy axis, E_g was obtained.

spheroid or ellipsoid, we used the Fura Kara effective field theory to get the optimal condition of poling.[11] Under external poling electric field E_p, the effective electric-field intensity E that acts on isolated crystals in composite thin films can be given as

$$\frac{E}{E_p} = \frac{2\epsilon_1}{2\epsilon_1 + \epsilon_2 + \phi(\epsilon_1 - \epsilon_2)}, \tag{1}$$

where ϵ_1 and ϵ_2 are the dielectric constants of PC and BT, respectively. ϕ is the volume ratio of BT in thin films. Figure 3 displays the temperature dependence of the dielectric constants of BT films, PC, and BT/PC films at 10 kHz. Here, BT films with grains of $\sim40-50$ nm were prepared by sol gel.[12]

The dielectric constant of PC rises very fast near $T_g(\sim160\ °C)$. The dielectric constant of pure BT increases slowly until the temperature reaches 100 °C near the Curie point of BT. From the range of values ϵ_1 and ϵ_2 measured over the temperature range of 30–165 °C and formula (1), the relationship of E/E_p vs ϵ_1 and ϵ_2 can be obtained, as shown in the three-dimensional graph of Fig. 4. We can see that the E/E_p increases fast after 100 °C and reaches the maximum value at about 165 °C, near the T_g of PC. Due to plasticization, the T_g of the BT/PC composite thin film is a little lower than the T_g of PC. So the optimum poling temperature in this paper was 160 °C.

The unpoled BT/PC composite thin films show higher transparency in the range of 300–800 nm ($\sim70\%$). The transmittance of the poled films is lower than that of the unpoled ones due to the alignment of BT nanocrystals, as
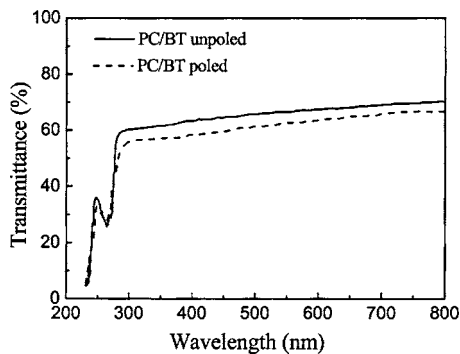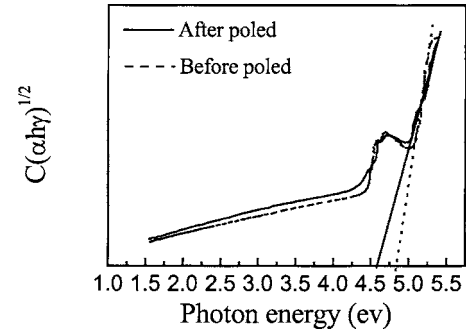
seen in Fig. 5. The optical band gap of poled and unpoled films can be calculated by using the intercept method and the following formula:

$$\alpha = \frac{1}{d}\ln\left(\frac{1}{T}\right) \quad \text{and} (\alpha\ h\nu)^{1/2} \propto (h\nu - E_g), \tag{2}$$

where $d=1.2\ \mu m$, α is the absorption coefficient near the absorption edge, and T is the transmittance of the films.[13] The optical band gap of unpoled BT/PC and poled BT/PC is calculated to be 4.82 and 4.58 eV, as shown in Fig. 6. The decrease of E_g indicates that the optical band gap E_g depends mainly on the states of the orientations of BT nanocrystals in the composite thin films. Figure 7 exhibits a photograph of a 10-wt % BT-doped BT/PC composite film on a 2×2-cm^2 fused quartz. We can prepare high transparency and uniform composite films in a relatively large area.

The modified setup using a stabilized He-Ne laser (632.8 nm) was used to measure the EO coefficients of poled BT/PC composite films, as shown in Fig. 8.[14] A chopper was used to modulate the laser density. A direct current (dc) field was applied to the sample. The electric field has a 45° angle to the polarization of incident light. The electric component of the light can thus be divided into two equal components, which is parallel and perpendicular to the applied electric field, respectively. After the analyzer converts the retardation to intensity variation, a photodiode is used to detect the output intensity that can be expressed as

FIG. 5. Transmission spectra of BT/PC composite films before and after poling.
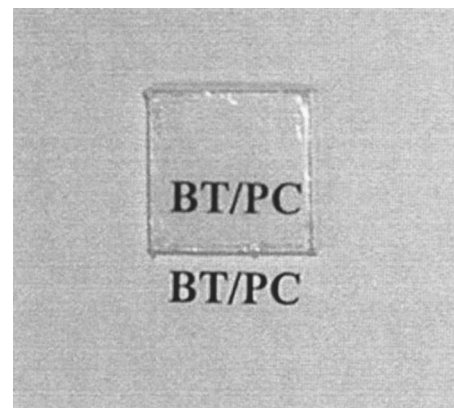

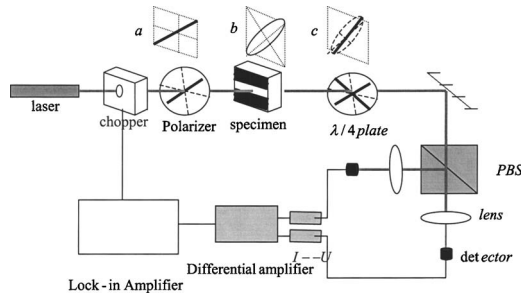FIG. 7. The photograph of 10-wt % BT-nanocrystal-doped composite film.

FIG. 8. Setup for ellipsometric measurements of electro-optic effect of BT/PC films.

$$I = \frac{I_0}{2}(1 + \Gamma), \qquad (3)$$

$$\Gamma = \frac{1}{2}n^3 k d \gamma E, \qquad (4)$$

$$\Delta n = \frac{\Delta \delta}{kd} = \left(\frac{2I - I_0}{I_0}\right)\frac{\lambda}{2\pi d}, \qquad (5)$$

$$\gamma = \left(\frac{2I - I_0}{I_0}\right)\frac{\lambda D}{n^3 \pi d V}, \qquad (6)$$

where Γ is the pure EO-induced retardation, $k = 2\pi/\lambda$, and $\Delta \delta$ is the phase delay value. Defining γ as the effective linear EO coefficients and neglecting the higher order EO effect, n is the refractive index of the sample, and d the film thickness. E is given by V/D, where D is the electrode spacing. I is detected by a lock-in amplifier.

The effective linear EO coefficients of poled BT/PC composite films on fused quartz were detected using the experiment setup illustrated in Fig. 8. Figure 9 plots the curves of birefringence shift (Δn) of poled BT/PC films on fused quartz as a function of applied electric field. The corresponding effective EO coefficients and figures of merit are summarized in Table I. The 20-wt % BT-nanocrystal-doped composite films had the largest figure of $\Delta n/E$, slightly larger than that of the 10-wt % BT-doped composite film and much larger than that of 5-wt % BT-doped composite film, showing the strongest EO properties in the three kinds of composite films. By calculation, the average effective linear EO coefficients γ of 5-, 10-, and 20-wt % BT-doped composite
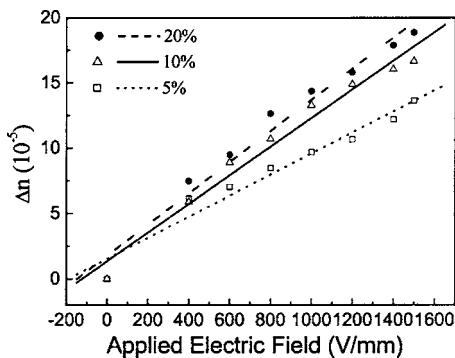

FIG. 9. Birefringence shift (Δn) of the BT/PC composite film as a function of applied electric field.

TABLE I. The γ and F_2 of BT/PC composite films with different concentrations of BT nanocrystals.

Doped BT content	0%	5%	10%	20%
γ(pm/V)	0.6	43.2	56.7	63.1
F_2(pm/V)	1.0	77.8	94.4	103.1

films are ~43.2, 56.7, and 63.1 pm/V, respectively, much larger than that of industry standard LiNbO$_3$ where $r33$ is 30 pm/V. Additionally, the figure of merit $F_2 = n^3\gamma/\epsilon$ is required to present a large value for EO devices. The F_2 value of the 5-, 10-, and 20-wt % BT-doped composite films BT/PC were estimated to be 77.8, 94.4, and 103.1 pm/V, respectively, comparing quite favorably with industry standard LiNbO$_3$ where F_2 is 12.8 pm/V. We can remark that even if their EO coefficients are not very large, the BT/PC composite polymer films show relatively large figures of merit owing to their very small value of the dielectric constant, which is 2.5 (10 wt %) at room temperature and the frequency of 10 kHz. The EO property of poled pure PC polymer films without doped BT nanocrytals was also measured for comparison, as listed in Table I. We can observe that linear EO coefficients and figures of merit of BT/PC films increased with the concentration of doped BT nanocrystals. The difference value between 20 and 10 wt % was smaller than that between 10 and 5 wt %. So though EO properties of such composite films can be further increased by increasing the concentration of the doped BT nanocrystals when the concentration of nanocrystals is low, they cannot be increased indefinitely due to the decrease of transparency caused by light scattering and aggregation of nanocrystals when the concentration of nanocrystals becomes high. It can be speculated that decreasing the size of doped nanocrystals will help to overcome these problems and improve the EO properties of composite films. This work is under way.

IV. CONCLUSION

Different concentrations BT-nanocrystals-doped uniform BT/PC composite thin films were prepared using spin-coating method. The pure perovskite tetragonal phase BT nanocrystals (~40–50 nm) were obtained by hydrothermal method. The structure, poling, band gap, and EO properties of composite films were investigated by means of various techniques. The electro-optic coefficient of 5-, 10-, and 20-wt % poled BT/PC composite polymer films is measured to be 43.2, 56.7, and 63.1 pm/V at 633 nm under room temperature. The figures of merit F_2 of these three types of composite films were estimated to be 77.8, 94.4, and 103.1 pm/V, respectively, much larger than that of industry standard LiNbO$_3$ crystal, indicating that this composite polymer film exhibits very good EO properties. In addition, the electro-optical properties of such composite polymer thin films can be further increased by increasing the concentration of the doped BT nanocrystals.

ACKNOWLEDGMENTS

[1] Y. L. Zhang, C. L. Mak, K. H. Wong, and C. L. Choy, Thin Solid Films **449**, 63 (2004).

[2] B. G. Potter, D. Dimos, M. B. Sinclair, and S. Lockwood, Integr. Ferroelectr. **11**, 59 (1995).

[3] K. D. Preston and G. H. Haertling, Appl. Phys. Lett. **60**, 2831 (1992).

[4] M. Zgonik, P. Bernasconi, M. Duelli, R. Schlesser, and P. Günter, Phys. Rev. B **50**, 5941 (1994).

[5] A. Petraru, J. Schubert, M. Schmid, and C. Buchal, Appl. Phys. Lett. **81**, 1375 (2002).

[6] B. H. Robinson *et al.*, Chem. Phys. **245**, 35 (1999).

[7] G. R. Meredith, J. V. Dusen, and D. J. Williams, Macromolecules **15**, 1385 (1982).

[8] S. R. Marder, B. Kippelen, A. K. Y. Jen, and N. Peyghambarian, Nature (London) **388**, 845 (1997).

[9] W. C. Liu, A. D. Li, J. Tan, D. Wu, H. Ye, and N. B. Ming, Appl. Phys. A: Mater. Sci. Process. (in press).

[10] S. Urek and M. Drofenik, J. Eur. Ceram. Soc. **18**, 279 (1998).

[11] K. T. Furu, J. K. Fu, and E. Fukada, Jpn. J. Appl. Phys. **15**, 2119 (1976).

[12] A. D. Li, C. Z. Ge, P. Lu, D. Wu, S. B. Xiong, and N. B. Ming, Appl. Phys. Lett. **70**, 1616 (1997).

[13] S. G. Lu, C. L. Mak, and K. H. Wong, J. Appl. Phys. **94**, 3422 (2003).

[14] J. W. Li, F. Duewer, C. Gao, H. Y. Chang, and X. D. Xiang, Appl. Phys. Lett. **76**, 769 (2000).